CSIRO PUBLISHING

Environ. Chem. **2018**, *15*, 259–266
https://doi.org/10.1071/EN17221

Research Paper

Abiotic reduction of insensitive munition compounds by sulfate green rust

Raju Khatiwada,[A] *Robert A. Root,*[A] *Leif Abrell,*[A,B] *Reyes Sierra-Alvarez,*[C] *James A. Field*[C] *and Jon Chorover*[A,B,D]

[A]Department of Soil, Water and Environmental Science, University of Arizona, Tucson, AZ 85721, USA.
[B]Arizona Laboratory for Emerging Contaminants, University of Arizona, Tucson, AZ 85721, USA.
[C]Department of Chemical and Environmental Engineering, University of Arizona, Tucson, AZ 85721, USA.
[D]Corresponding author. Email: chorover@email.arizona.edu

Environmental context. There is a growing need to understand how insensitive munitions compounds behave in natural environments, particularly in soils, where non-combusted residues accumulate. Here, we tested the ability of sulfate green rust, a naturally occurring mineral, to transform munitions compounds by reacting with the mineral surface. Our results show that both the munitions compounds and the mineral structures are transformed in an oxidation–reduction reaction that alters the compounds' environmental fates.

Abstract. Abiotic transformation of contaminants by redox-active mineral surfaces plays an important role in the fate and behaviour of pollutants in soils and sediments. However, there is very little information on such transformations for the insensitive munitions compounds (IMCs), 3-nitro-1,2,4-triazol-5-one (NTO) and 2,4-dinitroanisole (DNAN), developed in recent years to replace the traditional munition compounds in explosive mixtures. We tested the ability of sulfate green rust to transform NTO and DNAN (0.5 mM) under anoxic conditions at pH 8.4 in laboratory experiments, by using green rust supplied at 10 g kg^{-1} (w/w) solid concentration. Results indicate that NTO and DNAN underwent rapid abiotic reduction to their organic amine daughter products. NTO was completely transformed to 5-amino-1,2 4-triazol-3-one (ATO) within 20 min of reaction. This is the first report of NTO reduction by a naturally occurring mineral. Similarly, DNAN was rapidly transformed to 2-methoxy-5-nitroaniline (MENA) and 4-methoxy-5-nitroaniline (iMENA). The reduction occurred with an intriguing staggered regioselectivity. Over the first 10 min, the *para*-nitro group of DNAN was selectively reduced to generate iMENA. Thereafter, the *ortho*-nitro group was preferentially reduced, generating MENA. Both iMENA and MENA were subsequently transformed to the final reduction product 2,4-diaminoanisol (DAAN) within 1 day. Iron Kα X-ray absorption near-edge spectroscopy (XANES) studies of reacted solids indicated oxidative transformation of the green rust to lepidocrocite-like mineral forms. These results indicate that the IMCs can be rapidly transformed in soil, sediment or aquatic environments containing green rust.

Received 23 December 2017, accepted 5 April 2018, published online 2 August 2018

Introduction

The insensitive munition compounds 3-nitro-1,2,4-triazol-5-one (NTO) and 2,4-dinitroanisole (DNAN) are being increasingly utilised by departments of defence worldwide, which indicates a need to better understand their behaviour in environmental soil and water systems. Despite their lower risk of unintended detonation (Walsh et al. 2013), the environmental risk associated with these compounds is largely unknown. The high aqueous solubility of NTO is a major concern for groundwater contamination (Spear et al. 1989; Le Campion et al. 1999; Smith and Cliff 1999). DNAN does not readily undergo chemical or biological oxidation due to the electron-withdrawing nitro groups that make the benzene ring an electron deficient *pi*-electron system (Olivares et al. 2013; Shen et al. 2013; Ou et al. 2015*a*; Olivares et al. 2016). However, these compounds are readily reduced in suboxic soil by microbes (Olivares et al. 2013; Kennedy et al. 2015; Olivares et al. 2016). The initial reduction of nitro groups to amino groups is a key step in the (bio)transformation of these compounds in the natural environment and potentially in engineered remediation systems. The reduction of nitro groups to amines enables the further transformation of these reduced daughter products by both microbial and mineral-surface-mediated transformation. Various studies have suggested oxidative abiotic transformation of aromatic amines and heterocyclic amines upon reaction with surfaces of redox-active minerals, such as birnessite (Laha and Luthy 1990; Linker et al. 2015; Salter-Blanc et al. 2016). There have also been previous reports of abiotic DNAN transformation by using reduced iron, either in solution or adsorbed onto mineral surfaces (Niedzwiecka and Finneran 2015) and with zero valent iron (ZVI) (Boparai et al. 2010; Hawari et al. 2015; Ou et al. 2015*a*), but detailed information on transformation products is still lacking.

Green rust ($Fe^{II}_4\ Fe^{III}_2\ (OH)_{12}\ SO_4 \cdot 2H_2O$) is a layered double hydroxide composed of Fe^{II} and Fe^{III} hydroxide octahedral layers separated by interlayer water molecules and anions that may include sulfate, or carbonate, depending upon conditions of formation (Schwertmann and Cornell 1991: pp. 143–145). Green rust is a common, metastable intermediate formed by partial oxidation of Fe^{II} or partial reduction of Fe^{III} in supersaturated soil solutions, and it has also been observed as a biocorrosion product of ZVI or steel (Chaves 2005; Boparai et al. 2010; Yin et al. 2015). It has the potential to play an important role in the reductive transformation of various inorganic species (Hansen and Koch 1998; Chaves 2005; Skovbjerg et al. 2010) and organic contaminants (Refait et al. 2003; Elsner et al. 2004; Chun et al. 2007; Larese-Casanova and Scherer 2008; Boparai et al. 2010; Kone et al. 2011; Han et al. 2012; Chen et al. 2014), and may act as a potent reductant for the transformation of IMCs. Green rust (GR), which forms in redox dynamic environments comprising aqueous phase Fe^{II}, is capable of transforming some conventional compounds abiotically, including 2,4,6-trinitrotoluene (TNT), 1,3,5-trinitro-1,3,5-triazinane (RDX) and 1,3,5,7-tetranitro-1,3,5,7-tetrazocane (HMX) to various nitroso (RDX, HMX) and amino degradation products (TNT) (Boparai et al. 2010). However, the transformation of novel IMCs upon reaction with green rust has not been reported previously. Hence, there is a need to determine whether GR can promote the reductive transformation of IMCs in aqueous systems. Likewise, details are needed on the formation and identity of the reaction intermediates and products, both for the IMCs and the mineral reactants, over the course of the abiotic reduction process. Therefore, the ability of GR to transform NTO and DNAN to measurable products was tested in this study under laboratory conditions.

Experimental

Chemicals

3-Nitro-1,2,4-triazol-5-one (NTO; CAS # 932–64–9, >95 % purity) was purchased from Interchim (San Pedro, CA). 3-Amino-1,2,4-triazol-5-one (ATO; CAS #1003-35-6, >95 % purity) was purchased from Princeton BioMolecular Research, Inc. (Princeton, NJ). 2,4-Dinitroanisole (DNAN; CAS # 119-27-7, 98 % purity) was purchased from Alfa Aesar (Ward Hill, MA). 2-Methoxy-5-nitroaniline (MENA; CAS # 99-59–2, 98 % purity) and 2,4 diaminoanisole (DAAN; CAS# 615-05-4, 99.6 % purity) were purchased from Sigma-Aldrich (St Louis, MO). 4-Methoxy-5-nitroaniline (iMENA; CAS # 577-72-, 97 % purity) was obtained from Accela ChemBio (San Diego, CA, USA). Selected properties of IMC parent compounds are listed in Table 1.

Mineral synthesis

Sulfate green rust (GR) was synthesised by partial oxidation of $FeSO_4$ (Schwertmann and Cornell 1991: p. 104). Briefly, $FeSO_4$ solution (370 mL), freshly prepared from $FeSO_4 \cdot 7H_2O$, was purged with N_2 in a closed reaction vessel and titrated to pH 7.0. The N_2 was then replaced by CO_2-free air while the pH was maintained by using 1 M NaOH. After 40 min, the green precipitate was collected and stored in sealed amber bottles with N_2 in the headspace. The mineral stock concentration was 0.1 g mL^{-1}, as determined by air drying inside a glove box. The composition of the synthesised material was assessed by using X-ray diffraction (Supplementary Material).

Mineral-surface reactivity experiments

The capacity of GR to reduce NTO and DNAN was tested under anoxic conditions in a 25 mM Na_2SO_4 background electrolyte, using batch kinetic reactors situated inside a glove box. The background solution and IMC stock solutions were adjusted to pH 8.4. The reaction was conducted in a 10 mL syringe with a 0.2 μm filter attached to the outlet. The syringe contained GR and background electrolyte with 0.5 mM solutions of NTO or DNAN at an initial solid concentration of 10 g kg^{-1}. The syringe reactor was gently agitated on a horizontal shaker at 30 rpm inside the glove box for the duration of the reaction (3 h for NTO and 3 days for DNAN). Samples were collected at different time intervals between 0 to 3 h for NTO, and 0 to 3 days for DNAN reactors. When subsamples were collected, the reaction was halted by membrane filtration (0.2 μm filter). The subsamples were then analysed by ultra-high performance chromatography with photodiode array detection (UHPLC-PDA), as described below. Solids were transferred within the glove box into gas-impermeable storage containers to enable transport before undergoing off-site iron Kα X-ray absorption near-edge spectroscopy (XANES).

A separate set of experiments was conducted to enable XANES monitoring of iron-redox status and associated GR mineral speciation changes during the reaction. A closed-loop flow-through reaction cell was designed for monitoring GR oxidation in real time (Fig. S2, Supplementary Material). A cell (3 mL) was packed in an anaerobic chamber (Coy, MI) with IMC at a solid to solution ratio of 1:1000. The lower solid-phase concentration for these experiments was selected to enable detection of mineral transformation (i.e. >10 % iron redox-state change). Dissolved IMC was mixed with GR by pumping the IMC solution into the reaction cell by peristaltic pump at a flow rate of 2 mL min^{-1}. Dissolved IMC was purged with ultra-high purity $He_{(g)}$ before and during the reaction. A control-reaction cell was packed as above and treated with deionised water for >14.5 h to assess whether any Fe speciation change was observed in the absence of IMC. Since six moles of electrons are transferred per mole of NTO reduced to ATO, whereas 12 moles of electrons are transferred per mole of DNAN reduced to DAAN, the initial NTO and DNAN concentrations were set at 0.5 and 0.25 mM, respectively, for the flow through experiments, so that the rates of mineral transformation could be compared directly. All other reaction conditions were as for the batch reactions described above. Changes in Fe speciation were monitored every 7 min by XANES for 200 min for both reactions, and again at 320 min and 680 min for DNAN to check for completion or meta-stability.

Chemical and XANES analysis

Chemical concentrations in liquid samples were analysed by using UHPLC-PDA (Agilent 1200 Infinity Series, Santa Clara, CA). For NTO and ATO, 5 μL samples were injected into the mobile phase (1 mL min^{-1}) under the following v/v ratios of 0.1 % trifluoroacetic acid (TFA) aqueous buffer and acetonitrile: 0–3 min 100/0; 11 min 85/15; 15 min 50/50; 17 min 50/50; 19–20 min 100/0. A Hypercarb™ column (150 mm × 4.6 mm, 5 μm pore size) with guard column was used at 30 °C. NTO (ret. time 15 min) was quantified at 340 nm, and ATO (ret. time 9 min) was quantified at 216.5 nm. For DNAN, MENA, iMENA and DAAN, 5 μL samples were injected with a 40/60 % methanol/water isocratic mobile phase at 0.25 mL min^{-1} for 15 min. An RSLC E2 Acclaim Explosives column (2.1 × 100 mm,

Table 1. Selected properties of TNT, insensitive munition compounds and their daughter products

N.A., not applicable; N/A, not available; pK_a, acid dissociation constant; S_w, water solubility; K_{ow}, octanol–water partition coefficient

IMCs	Chemical name	Structure	Molecular weight	pK_a	S_w (mg L^{-1})	Log K_{ow}	Susceptibility to degradation
DNAN	2,4-dinitroanisole	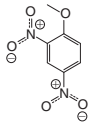	198.13	N.A.	213[A]	1.612[B]	EPA Biowin3 = 2.364 (weeks-months to degrade)[H], EPA Biowin7 = 0.2201[I]
MENA	2-methoxy-5-nitroaniline	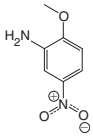	168.15	2.55[A]	252[A]	1.47[A]	N/A
iMENA	4-methoxy-5-nitroaniline	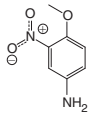	168.15	3.5[A]	4430[A]	0.8[A]	N/A
DAAN	2,4-diaminoanisole	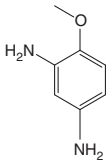	138.13	2.61(o)[A], 5.46(p)[A]	>40000[A]	<−1[A]	N/A
NTO	3-nitro-1,2,4-triazole-5-one	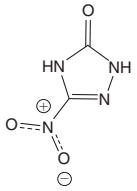	130.06	3.76[C]	12800[D]	0.21[E]	EPA Biowin3 = 2.914 (weeks to degrade)[H], EPA Biowin7 = 0.3984[I]
ATO	3-amino-1,2,4-triazole-5-one	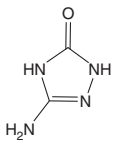	100.08	9.17–17.07[F]	11000[F]	N/A	N/A
TNT	2,4,6-trinitrotoluene	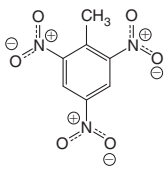	227.13	N.A	150[G]	1.86–2.00[G]	EPA Biowin3 = 2.281 (weeks-months to degrade)[H], EPA Biowin7 = −0.5924[I]

[A]Hawari et al. (2015), o = ortho, p = para; [B]Boddu et al. (2008); [C]Lee et al. (1987); [D]Smith and Cliff (1999); [E]Bhatnagar et al. (2013); [F]SciFinder (2018); [G]Rosenblatt et al. (1991); [H]EPA (2018*a*); [I]EPA (2018*b*).

particle size 2.2 µm; Thermo Scientific, Waltham, MA, USA) with guard column was used at room temperature. DNAN (ret. time 11 min) was quantified at 300 nm. MENA (ret. time 7 min), iMENA (ret. time 5 min) and DAAN (ret. time 2 min) were measured at 254 nm.

The solid-phase speciation change during the reaction was studied by using Fe K-edge synchrotron-based X-ray absorption near-edge spectroscopy (XANES) at the Stanford Synchrotron Radiation Lightsource (SSRL), Stanford, CA beam lines 11-2 and 4-3. The solid products formed at the end of the laboratory-based syringe reaction (3 h for NTO reactor and 3 days for DNAN reactor) were subjected to XANES analysis. Additionally, the continuous flow-through experiments were setup on Beamline 4-3 to measure Fe speciation every 7 min while dissolved IMC flowed through and mixed with solid GR (experimental details provided in the Supplementary Material). Normalised absorbance and first-derivative Fe-XANES spectra were used to study the shift in Fe oxidation state and coordination environment (Root et al. 2013). The XANES data were analysed by using SIXPack data analysis software (Webb 2005). Speciation was done using linear combination fitting (LCF). XANES spectra were analysed by fitting with binary linear

combinations using standard GR and lepidocrocite (Lp) spectra, while the weighting factors were forced to sum to unity. Details of XANES analysis are provided in the Supplementary Material.

Results and discussion

Both the parent compounds NTO and DNAN were susceptible to reduction by GR at 10 g kg^{-1} solid concentration in suspension (Fig. 1). NTO was reduced stoichiometrically to its corresponding amine daughter product, ATO, by GR (Fig. 1a). The reaction of NTO with GR was faster than that of DNAN. NTO had been largely reduced after 10 min and was not detectable after 20 min of reaction. This is the first report of NTO reduction by a naturally occurring mineral. The electron-withdrawing nitro group causes strong electron deficiency in the heterocyclic ring of NTO and surplus electron density on the nitro group, making the latter a favourable site for reduction by the structural Fe(II) of GR, leading to the transformation of NTO to ATO. Research conducted on NTO with bimetallic Fe/Cu and Fe/Ni solids at pH 3 and the same solid concentration used here suggest NTO loss from the solution within 1 h, but the reduction products were unclear (Koutsospyros et al. 2012; Kitcher et al. 2017). The product that we observed in our study, ATO, has also been observed to form from microbially mediated reduction of NTO (Le Campion et al. 1999; Krzmarzick et al. 2015; Madeira et al. 2017). In an anaerobic soil microcosm study with H_2 added as electron donor, a stoichiometrically consistent mass of ATO (95.3 %) was recovered from NTO biodegradation (Krzmarzick et al. 2015).

The other IMC, DNAN, was also reductively transformed, but more slowly, initially forming both iMENA and MENA. DNAN is predicted to be degraded more slowly than NTO, but faster than TNT, according to the BIOWIN model (Table 1). The observed reduction occurred with staggered regioselectivity. Over the first 10 min, the *para*-nitro group of DNAN was selectively reduced, generating iMENA. Thereafter, the *ortho* nitro group was preferentially reduced, generating MENA. Both iMENA and MENA were subsequently transformed to the final product DAAN within one day (Fig. 1b).

The initial biological reduction of DNAN has also been reported to be regioselective, but in the inverse sequence, favouring the nitro group in the *ortho* position to yield MENA (Platten et al. 2010; Perreault et al. 2012; Olivares et al. 2013; Olivares et al. 2016) before reduction of the second nitro group to yield DAAN (Platten et al. 2010; Olivares et al. 2013; Olivares et al. 2016). Previous studies evaluated DNAN reduction with ZVI, wherein it was converted to MENA (Ahn et al. 2011; Hawari et al. 2015; Ou et al. 2015*a*, 2015*b*), iMENA (Ahn et al. 2011; Ou et al. 2015*b*) and DAAN (Ahn et al. 2011; Ou et al. 2015*a*, 2015*b*; Hawari et al. 2015). Most of these studies report only a small fraction of iMENA products; the formation of MENA being favoured (Ou et al. 2015*b*; Hawari et al. 2015). However in the PAX-101 study, both MENA and iMENA were formed as important intermediates (Ahn et al. 2011), which suggests a non-regioselective reduction of both the *ortho*- and *para*-nitro groups of DNAN. The staggered regioselectivity of *para*- and *ortho*-nitro groups observed with GR is unique, and may relate to the stereochemistry of the adsorption complex. The relative differences in reduction of the nitro groups might be due to the methoxy-group substituent effect. Methoxy groups are electron donating, and the initial substitution favouring the *para* position over the *ortho* position may be due to steric hindrance by the methyl group upon surface reaction. Like

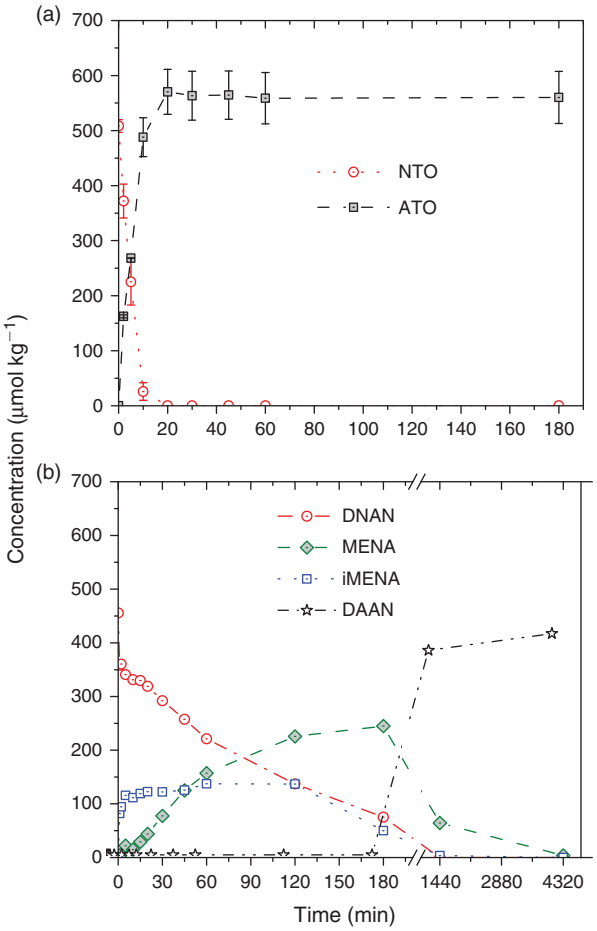

Fig. 1. Transformation of IMCs (a) NTO and (b) DNAN by sulfate GR in 10 g kg^{-1} suspension concentration at pH 8.4.

DNAN, other aromatic compounds with multiple nitro groups have a strongly electron-deficient carbon skeleton and increased electron density in the electron-withdrawing nitro groups, favouring their reductive biotransformation (Gorontzy et al. 1993; Hawari et al. 1998; Yang et al. 2008; Olivares et al. 2013).

The initial abiotic reduction of nitro groups to amines is a critical step in the (bio)transformation of IMCs because of the inherent resistance of IMCs to oxidation in oxic environments. Also, the oxidative biotransformation of reduced IMC daughter products has been observed in incubation studies in sludges (Olivares et al. 2013) and soils (Krzmarzick et al. 2015; Olivares et al. 2016). Therefore, initial reduction of the parent IMCs by GR is very important from an environmental remediation point of view.

The relative rates of reductive transformation observed in this study, albeit abiotic, are consistent with BIOWIN model predictions of biotic reduction rates. Higher values (Table 1) reflect greater susceptibility to (bio)transformation. Both models predict that NTO should degrade more rapidly than DNAN. Also, TNT is predicted to be more resistant to (bio)degradation than NTO and DNAN.

The normalised absorbance and first-derivative Fe-XANES spectra collected from reacted samples indicate that GR was oxidised to a lepidocrocite (γ -$Fe^{III}O(OH)$)-like species during reductive transformation of DNAN and NTO, which was more evident for NTO than for DNAN (Fig. 2; fit details in Table S1, Supplementary Material). Fe-XANES results show a clear

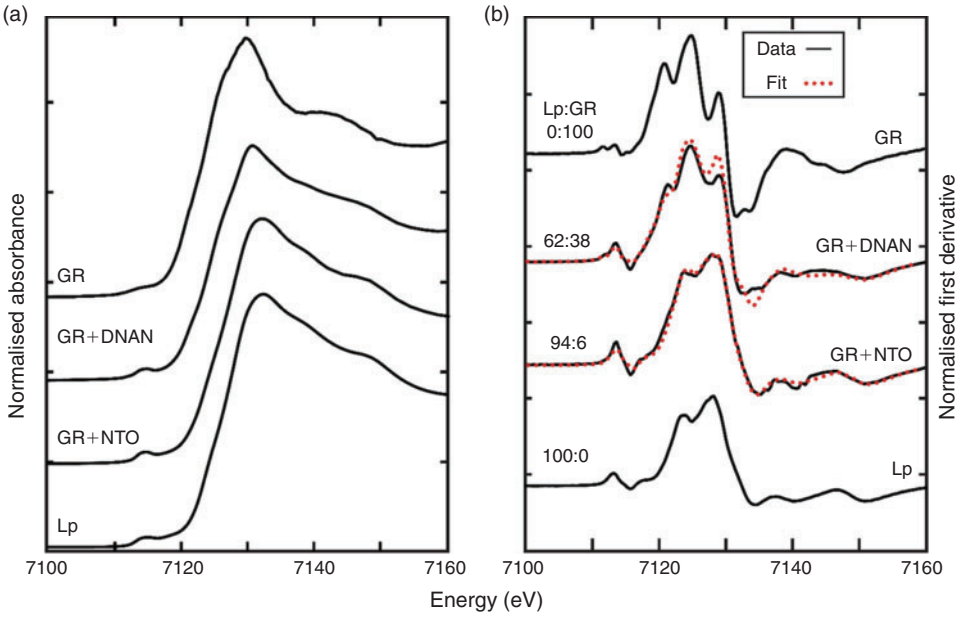

Fig. 2. (a) Normalised absorbance and (b) normalised first derivative Fe Kα XANES spectra of pre- and post-reaction sulfate GR (GR) with IMCs DNAN and NTO in batch reactions. Relative oxidation of GR and transformation to lepidocrocite (Lp) was examined by fractional convolution of reference spectra using linear combination fits (LCF) of reacted samples to reference compounds (fit details in Table S1, Supplementary Material). Data are shown in black, fractional fits are shown in dots. Results show a clear shift in oxidation state from mixed valent Fe^{II}/Fe^{III} (GR) to Fe^{III} (Lp) upon reaction with IMCs.

shift of oxidation state from Fe^{II}/Fe^{III} (GR) to Fe^{III} (lepidocrocite, Lp) upon reaction with the IMCs. However, the ratios of Lp to GR in these data from the batch experiments are several-fold higher than expected from stoichiometric considerations alone (i.e. 1.5 mol GR oxidised per mol NTO transformed to ATO or DNAN reduced to MENA). This result suggests that GR may be being further oxidised by an additional oxidant, most likely O_2 that somehow penetrated the storage vials following the reaction and before XAS analyses, despite attempts to prevent that.

Therefore, to avoid potential artefacts associated with post-reaction oxidation of GR, and to verify the solid-phase speciation change, we conducted a set of *in-situ* XAS experiments. In these flow-through experiments, the abiotic oxidative transformation of GR concomitant with reduction of both IMCs was observed in the reaction cell in real time (Fig. 3, fit details in Tables S2 and S3, Supplementary Material). Qualitatively consistent with the batch reactions, the Fe-XANES spectra collected during flow-through reaction show oxidation of GR to an Lp-like species during reductive transformation of both DNAN and NTO. In agreement with the analysis of the IMC and GR batch experiments, the oxidative transformation of the GR solids was faster with NTO than with DNAN; the GR and Lp reaching equal mass fractions after 73 min for NTO, and after 124 min for DNAN (Fig. 3). Further, the XANES LCF of the NTO-reacted GR in the flow-through system suggests that the Lp-like mineral phase accounted for 92 % of iron solids after 201 min; whereas ~78 % of the GR was oxidised by DNAN after 681 min (Fig. 3, fit details in Tables S2 and S3). These values are consistent with the stoichiometry of the reaction, which predicts more than 50 % conversion of GR to Lp in the quantitative conversion of NTO to ATO or DNAN to DAAN. Importantly, the control-reaction cell with GR present during flow through of the same background electrolyte solution but with no IMC, which was run for 885 min, showed no significant oxidation of GR (Fig. 3).

The batch (Fig. 1) and flow-through (Fig. 3) experiments were conducted with different experimental conditions and reactant/product species. However, consideration of electron equivalents enables inter-calibration of the datasets. Six mol of electrons are transferred per mol of NTO reduced to ATO, while 12 mol of electrons are required to reduce one mol of DNAN all the way to DAAN. Meanwhile, conversion of 1 mol of GR to 6 mol of Lp is associated with the loss of four mol of electrons (assuming four mol of Fe(II) and two mol of Fe(III), as in the standard formula for GR). Hence, 1.5 mol (3.0 mol) of GR are required per mole of NTO reduced to ATO (DNAN reduced to DAAN). The flow-through systems contained a total of 0.113 mmol of GR (accounting for initial Lp impurities) and 0.05 mmol of NTO (or 0.025 mmol of DNAN). Reduction of either the 0.05 mmol of NTO or the 0.025 mmol of DNAN required oxidation of 0.075 mmol (66 %) of the GR. Since the starting material contained ~25 % lepidocrocite by mass (Fig. 3), oxidation of 66 % of the GR (and presumably reduction of all of the NTO and DNAN) would be complete when χ_{GR} ~0.25. The times representing complete reduction of NTO to ATO and DNAN to DAAN can, therefore, be approximated by the intersection of the χ_{GR} data with the lower horizontal dashed lines in Fig. 3. These times are ~120 min for NTO (Fig. 3a) and 360 min for DNAN (Fig. 3b). The corresponding times for complete NTO and DNAN transformation to ATO and DAAN in the batch experiments were ~12 min (Fig. 1a) and 4320 min (Fig. 1b), respectively.

Hence, in the NTO case, where the IMC concentration was equivalent in the batch and flow-through experiments, a 10-fold lower GR concentration resulted in a corresponding 10-fold decrease in the NTO reduction rate, consistent with expectations for second-order kinetics. In the case of DNAN, the time to

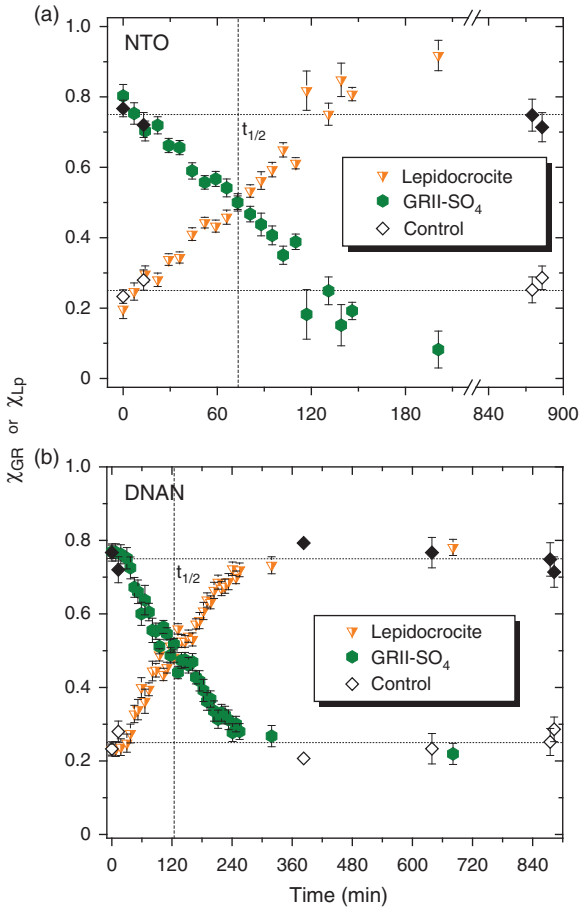

Fig. 3. IMC-induced transformation of GR to lepidocrocite (Lp). The time series abiotic oxidative transformation of GR to Lp upon reaction with IMC is shown for (a) NTO (0.5 mM) and (b) DNAN (0.25 mM). Mass-fractional components determined by LCF of Fe Kα XANES. The dashed vertical line indicates the point at which GR = Lp. Error bars represent the fractional-fit error (not replicate analyses).

achieve complete conversion to DAAN was ~12 times higher than in the batch study. This slightly greater difference between the batch and flow-through conversion times for DNAN than NTO is attributable to the fact that the initial DNAN concentration was 50% lower in the flow-through than in the batch experiment. In accordance with second order kinetics, a reduction in concentration of both reactants (when present at comparable stoichiometric concentrations, as is the case here) results in a corresponding further decrease in reaction rate.

These results are pertinent to the fate of IMCs in soils comprising GR, but they are also relevant to remediation systems employing zero valent iron (ZVI). GR has been previously observed as a reactive intermediate in ZVI contaminant removal systems (Refait et al. 2003; Satapanajaru et al. 2003; Chaves 2005; Boparai et al. 2010; Yin et al. 2012; Liu et al. 2014) with the eventual formation of Lp as the final end product of GR oxidation (Schwertmann and Fechter 1994; Liu et al. 2014). Additionally, sulfate GR was previously found to be transformed into an Lp-like form depending on pH and oxidation rate; on the other hand, the carbonate GR tends to form goethite-like Fe species (Carlson and Schwertmann 1990; Schwertmann and Fechter 1994), which are distinct in XAS spectra.

Conclusions

Iron(II) in sulfate GR can reductively transform IMCs to their respective amines under anoxic conditions at the expense of being oxidised to Fe(III) during the process. The current study is the first report of transformation of NTO by a naturally occurring mineral. During the process of GR Fe^{II} oxidation, the mineral is transformed to a lepidocrocite-like phase. The transformation of DNAN and NTO to reduced organic-amine daughter products, as mediated by the GR mineral surface, is of great importance for the geochemical transformation of these compounds in soil, since the initial reduction renders the molecule susceptible to subsequent oxidation accompanied by molecular fragmentation reactions. This study also provides insight into the mechanism of contaminant transformation by reaction with ZVI because GR is a major intermediate product that can drive further reductive transformation. Treatment of IMCs with GR may become an important remediation technique for abiotic transformation of munition compounds.

Supplementary material

The supplementary material includes: X-ray absorption spectroscopic (XAS) methods; X-ray diffractogram of sulfate green rust (Fig. S1); flow through X-ray absorption near edge structure set-up (Fig. S2); green rust control, reacted >14.5 h in flow through without IMC (Fig. S3); linear combination fits of green rust reacted with IMC (Table S1); linear combination XANES fits of green rust reacted with IMC NTO (Table S2); linear combination XANES fits of green rust reacted with IMC DNAN (Table S3).

Conflicts of interest

The authors declare no conflicts of interest.

Acknowledgements

This research was supported by the USA Department of Defense, Strategic Environmental Research and Development Program (SERDP) grant number ER-2221. Spectroscopic data were collected at the Stanford Synchrotron Radiation Laboratory (SSRL). Use of the SSRL, SLAC National Accelerator Laboratory, is supported by the USA Department of Energy, Office of Science, Office of Basic Energy Sciences under Contract No. DE-AC02-76SF00515.

References

Ahn SC, Cha DK, Kim BJ, Oh S-Y (2011). Detoxification of PAX-21 ammunitions wastewater by zero-valent iron for microbial reduction of perchlorate. *Journal of Hazardous Materials* **192**, 909–914. doi:10.1016/J.JHAZMAT.2011.05.104

Bhatnagar N, Kamath G, Potoff JJ (2013). Prediction of 1-octanol-water and air-water partition coefficients for nitro-aromatic compounds from molecular dynamics simulations. *Physical Chemistry Chemical Physics* **15**, 6467–6474. doi:10.1039/C3CP44284E

Boddu VM, Abburi K, Maloney SW, Damavarapu R (2008). Thermophysical properties of an insensitive munitions compound, 2,4-dinitroanisole. *Journal of Chemical & Engineering Data* **53**, 1120–1125. doi:10.1021/JE7006764

Boparai HK, Comfort SD, Satapanajaru T, Szecsody JE, Grossl PR, Shea PJ (2010). Abiotic transformation of high explosives by freshly precipitated iron minerals in aqueous Fe-II solutions. *Chemosphere* **79**, 865–872. doi:10.1016/J.CHEMOSPHERE.2010.02.037

Carlson L, Schwertmann U (1990). The effect of CO_2 and oxidation rate on the formation of goethite versus lepidocrocite from an Fe(II) system at pH-6 and pH-7. *Clay Minerals* **25**, 65–71. doi:10.1180/CLAYMIN.1990.025.1.07

Chaves LHG (2005). The role of green rust in the environment: A review. *Revista Brasileira de Engenharia Agrícola e Ambiental* **9**, 284–288. doi:10.1590/S1415-43662005000200021

Chen S, Fan D, Tratnyek PG (2014). Novel contaminant transformation pathways by abiotic reductants. *Environmental Science & Technology Letters* **1**, 432–436. doi:10.1021/EZ500268E

Chun CL, Hozalski RM, Arnold WA (2007). Degradation of disinfection byproducts by carbonate green rust. *Environmental Science & Technology* **41**, 1615–1621. doi:10.1021/ES061571F

Elsner M, Schwarzenbach RP, Haderlein SB (2004). Reactivity of Fe(II)-bearing minerals toward reductive transformation of organic contaminants. *Environmental Science & Technology* **38**, 799–807. doi:10.1021/ES0345569

EPA (2018*a*). 'Biowin3 – Ultimate Survey Model.' EPI Suite^{TM}-Estimation Program Interface.

EPA (2018*b*). 'Biowin7 – Anaerobic Linear Model.' EPI Suite^{TM}-Estimation Program Interface.

Gorontzy T, Kuver J, Blotevogel KH (1993). Microbial transformation of nitroaromatic compounds under anaerobic conditions. *Journal of General Microbiology* **139**, 1331–1336. doi:10.1099/00221287-139-6-1331

Han Y-S, Hyun SP, Jeong HY, Hayes KF (2012). Kinetic study of cis-dichloroethylene (cis-DCE) and vinyl chloride (VC) dechlorination using green rusts formed under varying conditions. *Water Research* **46**, 6339–6350. doi:10.1016/J.WATRES.2012.08.041

Hansen HCB, Koch CB (1998). Reduction of nitrate to ammonium by sulphate green rust: activation energy and reaction mechanism. *Clay Minerals* **33**, 87–101. doi:10.1180/000985598545453

Hawari J, Halasz A, Paquet L, Zhou E, Spencer B, Ampleman G, Thiboutot S (1998). Characterization of metabolites in the biotransformation of 2,4,6-trinitrotoluene with anaerobic sludge: Role of triaminotoluene. *Applied and Environmental Microbiology* **64**, 2200–2206.

Hawari J, Monteil-Rivera F, Perreault NN, Halasz A, Paquet L, Radovic-Hrapovic Z, Deschamps S, Thiboutot S, Ampleman G (2015). Environmental fate of 2,4-dinitroanisole (DNAN) and its reduced products. *Chemosphere* **119**, 16–23. doi:10.1016/J.CHEMOSPHERE.2014.05.047

Kennedy AJ, Laird JG, Lounds C, Gong P, Barker ND, Brasfield SM, Russell AL, Johnson MS (2015). Inter-and intraspecies chemical sensitivity: a case study using 2,4-dinitroanisole. *Environmental Toxicology and Chemistry* **34**, 402–411. doi:10.1002/ETC.2819

Kitcher E, Braida W, Koutsospyros A, Pavlov J, Su TL (2017). Characteristics and products of the reductive degradation of 3-nitro-1,2,4-triazol-5-one (NTO) and 2,4-dinitroanisole (DNAN) in a Fe-Cu bimetal system. *Environmental Science and Pollution Research International* **24**, 2744–2753. doi:10.1007/S11356-016-8053-7

Kone T., Hanna K., Usman M. (2011). Interactions of synthetic Fe(II)-Fe (III) green rusts with pentachlorophenol under various experimental conditions. *Colloids and Surfaces A - Physicochemical and Engineering Aspects* **385**, 152–158. doi:10.1016/J.JHAZMAT.2012.03.048

Koutsospyros A, Pavlov J, Fawcett J, Strickland D, Smolinski B, Braida W (2012). Degradation of high energetic and insensitive munitions compounds by Fe/Cu bimetal reduction. *Journal of Hazardous Materials* **219–220**, 75–81. doi:10.1016/J.JHAZMAT.2012.03.048

Krzmarzick MJ, Khatiwada R, Olivares CI, Abrell L, Sierra-Alvarez R, Chorover J, Field JA (2015). Biotransformation and degradation of the insensitive munitions compound, 3-nitro-1,2,4-triazol-5-one, by soil bacterial communities. *Environmental Science & Technology* **49**, 5681–5688. doi:10.1021/ACS.EST.5B00511

Laha S, Luthy RG (1990). Oxidation of aniline and other primary aromatic-amines by manganese-dioxide. *Environmental Science & Technology* **24**, 363–373. doi:10.1021/ES00073A012

Larese-Casanova P, Scherer MM (2008). Abiotic transformation of hexahydro-1,3,5-trinitro-1,3,5-triazine (RDX) by green rusts. *Environmental Science & Technology* **42**, 3975–3981. doi:10.1021/ES702390B

Le Campion L, Vandais A, Ouazzani J (1999). Microbial remediation of NTO in aqueous industrial wastes. *FEMS Microbiology Letters* **176**, 197–203. doi:10.1111/J.1574-6968.1999.TB13662.X

Lee KY, Chapman LB, Cobura MD (1987). 3-Nitro-1,2,4-triazol-5-one, a less sensitive explosive. *Journal of Energetic Materials* **5**, 27–33. doi:10.1080/07370658708012347

Linker BR, Khatiwada R, Perdrial N, Abrell L, Sierra-Alvarez R, Field JA, Chorover J (2015). Adsorption of novel insensitive munitions compounds at clay mineral and metal oxide surfaces. *Environmental Chemistry* **12**, 74–84. doi:10.1071/EN14065

Liu A, Liu J, Pan B, Zhang W-X (2014). Formation of lepidocrocite (gamma-FeOOH) from oxidation of nanoscale zero-valent iron (nZVI) in oxygenated water. *RSC Advances* **4**, 57377–57382. doi:10.1039/C4RA08988J

Madeira CL, Speet SA, Nieto CA, Abrell L, Chorover J, Sierra-Alvarez R, Field JA (2017). Sequential anaerobic-aerobic biodegradation of emerging insensitive munitions compound 3-nitro-1,2,4-triazol-5-one (NTO). *Chemosphere* **167**, 478–484. doi:10.1016/J.CHEMOSPHERE.2016.10.032

Niedzwiecka JB, Finneran KT (2015). Combined biological and abiotic reactions with iron and Fe(III)-reducing microorganisms for remediation of explosives and insensitive munitions (IM). *Environmental Science. Water Research & Technology* **1**, 34–39. doi:10.1039/C4EW00062E

Olivares C, Liang J, Abrell L, Sierra-Alvarez R, Field JA (2013). Pathways of reductive 2,4-dinitroanisole (DNAN) biotransformation in sludge. *Biotechnology and Bioengineering* **110**, 1595–1604. doi:10.1002/BIT.24820

Olivares CI, Abrell L, Khatiwada R, Chorover J, Sierra-Alvarez R, Field JA (2016). (Biol.)transformation of 2,4-dinitroanisole (DNAN) in soils. *Journal of Hazardous Materials* **304**, 214–221. doi:10.1016/J.JHAZMAT.2015.10.059

Ou C, Zhang S, Liu J, Shen J, Han W, Sun X, Lia J, Wang L (2015*a*). Enhanced reductive transformation of 2,4-dinitroanisole in a anaerobic system: the key role of zero valent iron. *RSC Advances* **5**, 75195–75203. doi:10.1039/C5RA11197H

Ou C, Zhang S, Liu J, Shen J, Liu Y, Sun X, Li J, Wang L (2015*b*). Removal of multi-substituted nitroaromatic pollutants by zero valent iron: a comparison of performance, kinetics, toxicity and mechanisms. *Physical Chemistry Chemical Physics* **17**, 22072–22078. doi:10.1039/C5CP02518D

Perreault NN, Manno D, Halasz A, Thiboutot S, Ampleman G, Hawari J (2012). Aerobic biotransformation of 2,4-dinitroanisole in soil and soil Bacillus sp. *Biodegradation* **23**, 287–295. doi:10.1007/S10532-011-9508-7

Platten WE, III, Bailey D, Suidan MT, Maloney SW (2010). Biological transformation pathways of 2,4-dinitro anisole and N-methyl paranitro aniline in anaerobic fluidized-bed bioreactors. *Chemosphere* **81**, 1131–1136. doi:10.1016/J.CHEMOSPHERE.2010.08.044

Refait P, Gehin A, Abdelmoula M, Genin JMR (2003). Coprecipitation thermodynamics of iron(II-III) hydroxysulphate green rust from Fe(II) and Fe(III) salts. *Corrosion Science* **45**, 659–676. doi:10.1016/S0010-938X(02)00138-5

Root RA, Fathordoobadi S, Alday F, Ela W, Chorover J (2013). Microscale speciation of arsenic and iron in ferric-based sorbents subjected to simulated landfill conditions. *Environmental Science & Technology* **47**, 12992–13000. doi:10.1021/ES402083H

Rosenblatt DH, Burrows EP, Mitchell WR, Parmer DL (1991). 'Organic explosives and related compounds. Part G.' (Springer-Verlag: Berlin Heidelberg)

Salter-Blanc AJ, Bylaska EJ, Lyon MA, Ness SC, Tratnyek PG (2016). Structure-activity relationships for rates of aromatic amine oxidation by manganese dioxide. *Environmental Science & Technology* **50**, 5094–5102. doi:10.1021/ACS.EST.6B00924

Satapanajaru T, Shea PJ, Comfort SD, Roh Y (2003). Green rust and iron oxide formation influences metolachlor dechlorination during zerovalent iron treatment. *Environmental Science & Technology* **37**, 5219–5227. doi:10.1021/ES0303485

Schwertmann, U, Cornell, RM (1991). 'Iron oxides in the laboratory. Preparation and characterization.' (VCH Editions: Weinhein, Germany).

Schwertmann U, Fechter H (1994). The formation of green rust and its transformation to lepidocrocite. *Clay Mineralogy* **29**, 87–98.

SciFinder (2018). Properties of 3-amino-1,2,4-triazole-5-one 3-amino-1,2,4-triazole-5-one (ATO) calculated using Advanced Chemistry Development (ACD/Labs) Software V11.02 (© 1994–2018 ACD/Labs).

Shen J, Ou C, Zhou Z, Chen J, Fang K, Sun X, Li J, Zhou L, Wang L (2013). Pretreatment of 2,4-dinitroanisole (DNAN) producing wastewater using

a combined zero-valent iron (ZVI) reduction and Fenton oxidation process. *Journal of Hazardous Materials* **260**, 993–1000. doi:10.1016/J.JHAZMAT.2013.07.003

Skovbjerg LL, Christiansen BC, Nedel S, Dideriksen K, Stipp SLS (2010). The role of green rust in the migration of radionuclides: An overview of processes that can control mobility of radioactive elements in the environment using as examples Np, Se and Cr. *Radiochimica Acta* **98**, 607–612. doi:10.1524/RACT.2010.1760

Smith MW, Cliff MD (1999). 'NTO-based explosive formulations: a technology review.' (DTSO Aeronautical Maritime Research Laboratory: Melbourne)

Spear, R. J., Louey, C. N., Wolfson, M. G. (1989). 'A preliminary assessment of 3-nitro-1,2,4-triazol-5-one (NTO) as an insensitive high explosive. (No. MRL-TR-89-18).' Materials Research Labs Ascot Vale (Australia), 38.

Walsh MR, Walsh ME, Taylor S, Ramsey CA, Ringelberg DB, Zufelt JE, Thiboutot S, Ampleman G, Diaz E (2013). Characterization of PAX-21 insensitive munition detonation residues. *Propellants, Explosives, Pyrotechnics* **38**, 399–409. doi:10.1002/PREP.201200150

Webb SM (2005). SixPACK: a graphical user interface for XAS analysis using IFEFFIT. *Physica Scripta* **T115**, 1011–1014. doi:10.1238/PHYSICA.TOPICAL.115A01011

Yang H, Halasz A, Zhao TS, Monteil-Rivera F, Hawari J (2008). Experimental evidence for in situ natural attenuation of 2,4-and 2,6-dinitrotoluene in marine sediment. *Chemosphere* **70**, 791–799. doi:10.1016/J.CHEMOSPHERE.2007.07.014

Yin W, Wu J, Li P, Lin G, Wang X, Zhu B, Yang B (2012). Reductive transformation of pentachloronitrobenzene by zero-valent iron and mixed anaerobic culture. *Chemical Engineering Journal* **210**, 309–315. doi:10.1016/J.CEJ.2012.09.003

Yin W, Wu J, Huang W, Wei C (2015). Enhanced nitrobenzene removal and column longevity by coupled abiotic and biotic processes in zero-valent iron column. *Chemical Engineering Journal* **259**, 417–423. doi:10.1016/J.CEJ.2014.08.040

Handling Editor: Enzo Lombi